63-3-3

SOLID ROCKET PLANT

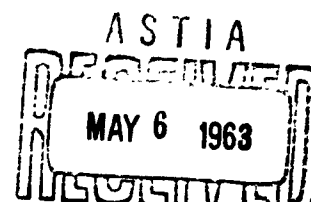ACOUSTICAL ANALYSIS OF
FILAMENT-WOUND POLARIS CHAMBERS

Contract NOw 62-1007c(FBM)

Bimonthly Progress Report No. 4

Report 0672-01 BM-4   25 March 1963

AEROJET
GENERAL TIRE
GENERAL

$(5) - 13 \overline{3} 6 \omega)$

(11) 25 March 1963

(7) N.A.
(8) u
(10) See m. p.p.
(12) 8 p
(13) N.A.
(16) N.A.
(17) N.A.
(18) N.A.
(19) N.A.

Rept
*) Report 0672-01BM-4

(6) ACOUSTICAL ANALYSIS OF FILAMENT-
WOUND POLARIS CHAMBERS

(15) Contract NOw 62-1007c (FBM)

$4. C.$

(9) Bimonthly Progress Report No. 4.

AEROJET-GENERAL CORPORATION
A SUBSIDIARY OF THE GENERAL TIRE & RUBBER COMPANY

PREFACE

This report was prepared by C. S. Lockman, Test Engineer, and its technical content approved by A. T. Green, Group Supervisor, both of the Special Projects Group, Structural Test Department.

ABSTRACT

This is the fourth bimonthly progress report on the program to investigate the aspects of acoustically analyzing Polaris filament-wound chambers; the progress accomplished during this report period is described herein.

TABLE OF CONTENTS

TABLE LIST

FIGURE LIST

FIGURE LIST (cont.)

APPENDIXES

I. OBJECTIVES

The objectives of this program are: (1) to develop sound-recording procedures so that the significance of sounds emanating from first-stage Polaris Model A3 chambers during hydrostatic testing may be determined and (2) to determine experimentally the velocity of sound in a composite material of glass filaments and resin, and the effect of filament-winding direction and superimposed stress fields on that velocity.

Because of basic differences in the objectives, the program is divided into two phases:

A. PHASE I

In Phase I, work is being directed toward the achievement of the first objective so that a noise envelope can be established that will show margins of typical behavior for a structurally sound chamber.

B. PHASE II

Work in Phase II is being directed toward the achievement of the velocity-of-sound objective so that knowledge obtained from the development work can ultimately be used to establish the location of noise sources by triangulation techniques.

II. SUMMARY

This report includes a discussion of the data-presentation and data-evaluation techniques, presents the test data obtained to date for both test objectives, and describes the data-acquisition and playback systems and their application. Results from Phase I testing show that there is a significant relationship between the sounds emanating from a filament-wound chamber

II, Summary (cont.)

during hydrostatic testing and the structural integrity of the chamber. The
measured acceleration amplitude (rms) during hydrostatic testing is a function
of chamber burst pressure and, as the data show, is inversely related to the
burst pressure. (Figure 1).

Comparative data for three chambers tested to both the proof and burst
pressure demonstrated the sensitivity of the accelerometer techniques of
measurement.

The results of Phase II testing (Table 1) show that the velocity of sound
in the forward and aft heads and in the cylindrical section of Polaris Model A3X
chambers differs (9314, 11, 294, and 10, 608 ft/sec, respectively). These data
also show that the direction of filament-winding and superimposed stress fields
do not affect the velocity of sound through a Polaris Model A3X chamber of
resin-impregnated E-HTS glass roving.

III.   TECHNICAL DISCUSSION

    A.   PHASE I

        1.   Data Presentation

            The data reported are presented in three-dimensional plots
and in tabulated form. The three-dimensional surface plots of acceleration
magnitude (Figures 2 through 5) display the frequency of chamber acceleration
and the amplitude components as a function of hydrostatic chamber pressure.
The individual frequency-amplitude plots define the magnitude surface for
any of the amplitude levels along the axis of frequencies. The tabulated data
include average g-acceleration amplitudes to show relative levels between
similar accelerometer functions from different tests.

III, A, Phase I (cont.)

The three-dimensional plots are presented to show the relationship between acceleration amplitude and frequency components as a function of hydrostatic pressure. The plots are composed of six individual Brüel-and-Kjaer filtered-data traces. The traces are shown in line spectra along the frequency axis. The traces have a common amplitude scale in terms of acceleration units (g) and in power spectral density units (g^2/cps). The composite signal amplitude for all frequencies may be read either in g units or in g^2/cps over the entire frequency spectrum. The acceleration amplitude over any portion of the frequency spectrum may be determined from the g^2/cps scaling factor. The acceleration amplitude over the frequency spectrum from 200 to 8000 cps is determined by reading the g^2/cps amplitude and calculating as follows:

$$g(rms) \text{ overall (from 200 to 8000 cps)} = \left[(g^2/cps)\,(8000 - 200) \right]^{1/2}$$

The above g amplitude is equivalent to the overall g level read from the composite signal amplitude.

The data in Table 2 are presented to show the relative average acceleration units (g) between similar accelerometer locations on different chambers. The g-psi units are derived from measuring the area of the g(rms)-psi composite data plots as obtained on a graphic sound-level recorder. The average g units are then derived by dividing the g-psi area by the overall pressure increment.

2. Data Analysis Technique

The accelerometer data obtained during hydrostatic tests will show (if evaluated in terms of average acceleration amplitude and transient impulse sequence over a pressure cycle) the relative structural integrity of a particular chamber. The acceleration history for a series of hydrostatically pressure-tested chambers will show a range of acceleration amplitudes and impulse densities that may be used for comparative data analysis (Figures 2, 3, 4, and 5).

III, A, Phase I (cont.)

       The acceleration data obtained during hydrostatic tests are being evaluated by comparing the average acceleration amplitudes, impulse densities, and burst pressures from a series of tests. The acceleration history from a series of burst-pressure cycles will demonstrate a relationship between acceleration amplitude and burst pressure (Figure 1). The data from hydrostatic proof- and burst-pressure cycles are being evaluated to develop the relationship between the acceleration amplitude and burst pressure. The respective acceleration data for the burst and proof cycles are being correlated to establish a relationship between the relative acceleration amplitudes of these test cycles. Ten to twenty chambers will be thus evaluated to establish the relationship between acceleration amplitude during proof-pressure testing to 945 psi and the ultimate burst pressure so that the ultimate burst pressure can be predicted. The foregoing technique will also be used to predict the burst pressure from acceleration amplitudes at pressure increments below 945 psig.

       3.   Test Results

       Representative accelerometer-amplitude data from all chambers tested with accelerometer instrumentation are shown in Table 2. Although all hydrostatically tested chambers were instrumented with multiple accelerometers, as shown in Figure 6, only two accelerometer amplitudes, representative for all acceleration levels, are tabulated.

       Only three chambers have been hydrostatically tested to the proof pressure and to burst after accelerometers were incorporated into the instrumentation requirements for pressure tests. Data from these tests (646P, 645P, and 779P) show a higher average acceleration amplitude for lower burst pressures (Figure 1). However, as shown in Figure 1, there actually were four chambers that had accelerometers installed near the burst area. Three of these chambers (tests 646P, 645P, and 784P) burst in the aft head, whereas the fourth chamber (test 779P) burst in the cylindrical

III, A, Phase I (cont.)

section. A comparison of average acceleration amplitudes vs burst-pressure increment, measured at accelerometer station G105 (Figure 1) for the former three tests and at accelerometer station G110 (Figure 1) for the latter test, shows a relatively linear relationship between acceleration amplitude and burst pressure. A comparison of average acceleration amplitudes from the proof-pressure increments vs burst pressure shows a nonlinear relationship (Figure 1).

Burst tests 478P, 686P, and 479P do not show a linear relationship between acceleration amplitude and pressure (Table 2). The first two tests do not show this relationship because the chambers burst in the forward head, which was not instrumented with accelerometers. The latter test (479P) does not show correlative accelerometer data because it had been pressurized to 1400 psig in an earlier attempted burst test (which was conducted prior to the inception of the acoustic program).

B.   PHASE II

1.   Velocity-of-Sound Measurements

The velocity-of-sound measurements made on AISI-4130 steel were within 5% of the theoretically calculated values. The velocity-of-sound measurements made on small filament-wound samples showed that the measurements were not repeatable. The cause for the nonrepeatability in small samples is attributed to the short distances between accelerometers and to the variance in impact points.

The limited success of measuring the velocity of sound through small samples led to sound measurements on a full-scale chamber. A water-filled Polaris Model A3X chamber made of resin-impregnated E-HTS roving

III, B, Phase II (cont.)

was shock-impulse tested to determine the velocity of sound through the three separate chamber subsections. The cylindrical section, and the aft as forward heads were independently shocked, and velocity-of-sound measurements were made at various angles relative to filament wrap. The results of this testing revealed that the velocity of sound did not change relative to the angle of wrap.

The chamber was then installed in a test cell and velocity-of-sound measurements were made at hydrostatic chamber pressures of 0, 300, 500, and 700 psig. The chamber, instrumented along its length with eight accelerometers (Figure 7), was shock-impacted at the polar plug of the aft head. The shock-impulse measurements at various hydrostatic pressures show that the velocity of sound did not change with pressure. However, the shock-impulse amplitudes were found to vary as the hydrostatic pressure changed. The data indicate a higher impulse-amplitude transfer with increased chamber pressure, as shown in Table 3 for pressures between 0 and 700 psig.

All velocity-of-sound measurements determined from shock-impulse testing on the full-scale filament-wound chamber are shown in Table 1, including the range of measurements and the calculated standard deviations on the three separate chamber subsections. The relationship for the calculated standard deviation is also presented.

2. Status of Phase II Work

The program to measure the velocity-of-sound in glass-resin composites was completed except for additional analyses to ascertain the accuracy of the measurement system. The velocity-of-sound measurements presented in this report are based on about 50% of the reduced data. The standard deviation calculated on the basis of the remaining data may change the values presented.

IV. FUTURE WORK

A. APPLICATION OF VELOCITY-OF-SOUND MEASUREMENTS

The velocity-of-sound measurements already recorded and reduced will be further analyzed to determine the accuracy of measurements. The nominal velocity values obtained on the three separate chamber sections will be used to determine, by triangulation, the source of energy release during hydrostatic testing.

B. RECORDING OF DATA DURING HYDROSTATIC TESTS

The data recorded during hydrostatic proof-pressure and burst tests will continue to be processed and analyzed until the relationship between acceleration impulse-amplitude history and burst pressure has been determined (Figure 8).

The playback of these data through the Brüel and Kjaer equipment will continue; however, greater emphasis will be directed toward determining the acceleration impulse-amplitude history over the first 500 psig of the 945-psig hydrostatic proof-pressure cycle. This will allow determination of the structural integrity of a chamber at a proof pressure lower than 945 psig.

The acceleration data will be played through an electronic pulse-counter system that will count the total number of acceleration impulses of discrete amplitudes over a pressure-cycle increment. The total number of acceleration-impulse counts at four or five individual amplitude levels would define the acceleration-amplitude history over a given pressure increment. These data can then be used to define chamber integrity. The development of this technique will allow the monitoring of acceleration data through the electronic counter in real time.

IV, B, Recording of Data During Hydrostatic Tests (cont.)

The location of accelerometers used in hydrostatic tests will be slightly modified to include two forward-head accelerometers, which will record an acceleration sequence that may be used to determine the integrity of the forward head. This will ensure that a chamber will not be accepted on the basis of low-acceleration amplitudes that were measured only for the aft head.

A specially constructed Polaris Model A3X chamber will be hydrostatically tested in the near future. This chamber was constructed with strain gages positioned between the wraps to determine the interlaminar strains during hydrostatic tests and structural loadings. The chamber will be instrumented at the standard accelerometer locations that are used in the acoustical program. All strain data will be correlated directly with the acoustic data. The structural significance of the acoustic data will then be interpreted in terms of chamber strains.

C. ACOUSTIC MEASUREMENTS, ULTRASONIC TRANSLATOR

Various chambers, instrumented with accelerometers and with Model 114 ultrasonic translators of the Delcon Corp., will be hydrostatically tested. Chambers instrumented with Delcon ultrasonic translators are tested in a Polaris reliability program. The data obtained from this program will be published in a separate report.

TABLE 1

VELOCITY-OF-SOUND TABULATION FOR POLARIS MODEL A3X CHAMBERS

	CHAMBER SECTION		
	AFT	CYLINDER	FORWARD
n	12	41	14
R	1268 ft/sec	2236 ft/sec	1480 ft/sec
$\bar{y}$	11,294 ft/sec	10608 ft/sec	9,314 ft/sec
$P\{\bar{y}\}=.95$	11,026 ft/sec ≤ $\bar{y}$ ≤ 11,562 ft/sec	10,400 ft/sec ≤ $\bar{y}$ ≤ 10,816 ft/sec	9,036 ft/sec ≤ $\bar{y}$ ≤ 9,592 ft/sec
s^2	161,604 ft²/sec²	421,649 ft²/sec²	222,784 ft²/sec²
s	402 ft/sec	657 ft/sec	472 ft/sec

STATISTICS USED

n = sample size
R = sample range = (highest value - lowest value)

$\bar{y} = \frac{\Sigma}{n} x_i / n$ = sample mean

$P\{\bar{Y}\} = .95 = 95\%$ confidence interval for population mean $\bar{Y}$.

$$= Pr\left\{ \bar{y} - t_{(\alpha/2,n-1)} \frac{s}{\sqrt{n}} \leqslant \bar{Y} \leqslant \bar{y} + t_{(\alpha/2,n-1)} \frac{s}{\sqrt{n}} \right\}$$

s^2 = sample variance = $\dfrac{n \sum\limits_i^n x_i^2 - (\Sigma x_i)^2}{n(n-1)}$

* = sample standard error = $c\sqrt{s^2}$ where if n = 41 then c = 1.007
    n = 14 then c = 1.022
    n = 12 then c = 1.025

* for explanation of correction factor see STATISTICAL THEORY WITH ENGINEERING APPLICATION, A. Hald, pp 299, 300; John Wiley and Sons Inc., New York, 1952.

Table 1

TABLE 2

HYDROSTATIC TEST ACCELERATION HISTORY

Test	Chamber SN	Chamber Type	Accelerometer Location	Pressure Acceleration Area, G-psi	Pressure Increment, psi	Average Acceleration Amplitude, G rms	Chamber Failure Area (Section)
646 Proof	715085	E-HTS Glass USP-787 Resin	G105 G109	1600 660	945	1.7 0.7	
590 Proof	717068	E-HTS Glass USP-787 Resin	G105 G109	850 850	945	0.9 0.9	
723 Proof	717069	E-HTS Glass USP-787 Resin	G105 G109	190 190	945	0.2 0.2	
645 Proof	715086	S-994 Glass 58-68R Shell Resin	G105 G109	380 380	945	0.7 0.7	
755 Proof	711014	S-994 Glass USP/Shell Resin	G105 G109	190 190	945	0.2 0.2	
769 Proof	711014	S-994 Glass Shell Resin	G105 G109	1510 945	945	1.6 1.0	
779 Proof	717072	S-994 Glass USP/Shell Resin	G105 G109 G110	190 190 190	945	0.2 0.2 0.2	
646 Burst	715085	E-HTS Glass USP-787 Resin	G105 G109	510 392	392 (1337-945)	1.3 1.0	Aft Closure
686 Burst	711025	E-HTS Glass USP-787 Resin	G105 G109	80 105	265 (1210-945)	0.3 0.4	Forward Closure
478 Burst	711012	E-HTS Glass USP-787 Resin	G105	206	258 1203-945	0.8	Forward Closure
784 Burst	711008	E-HTS Glass USP-787 Resin	G105 G109	348 348	245 (1190-945)	1.5 1.5	Aft Closure
645 Burst	715086	S-994 Glass Shell Resin	G105 G109	475 238	475 (1420-945)	1.0 0.5	Aft Closure
479 Burst	717061	S-994 Glass Shell Resin	G105 G109	100 100	500 (1445-945)	0.2 0.2	Aft Closure
779 Burst	717072	S-994 Glass USP/Shell Resin	G105 G109 G110	231 231 231	770 (1715-945)	0.3 0.3 0.3	Center of Cylindrical Section

Table 2

TABLE 3

SHOCK-IMPULSE DAMPING CHARACTERISTICS
IN FILAMENT-WOUND CHAMBERS

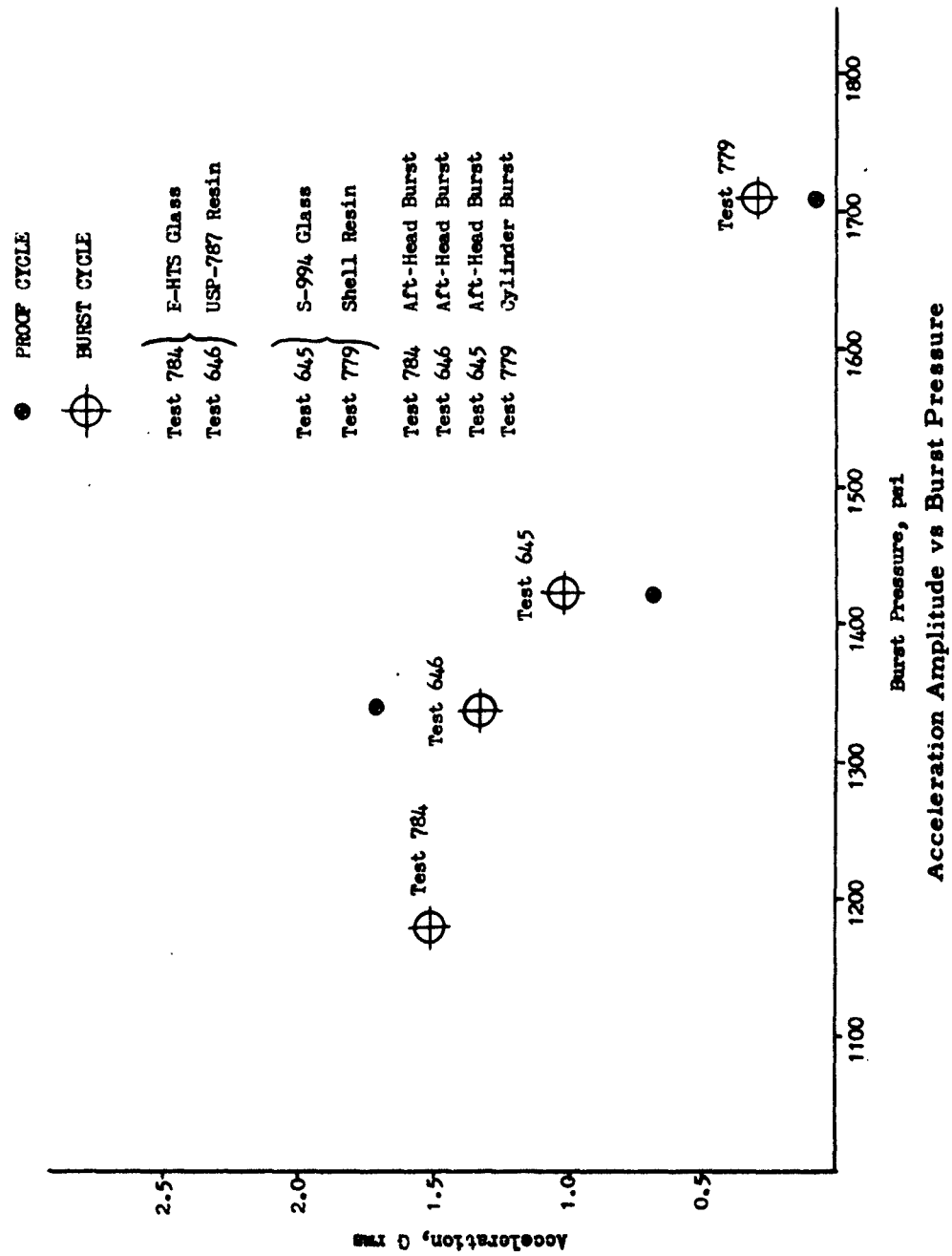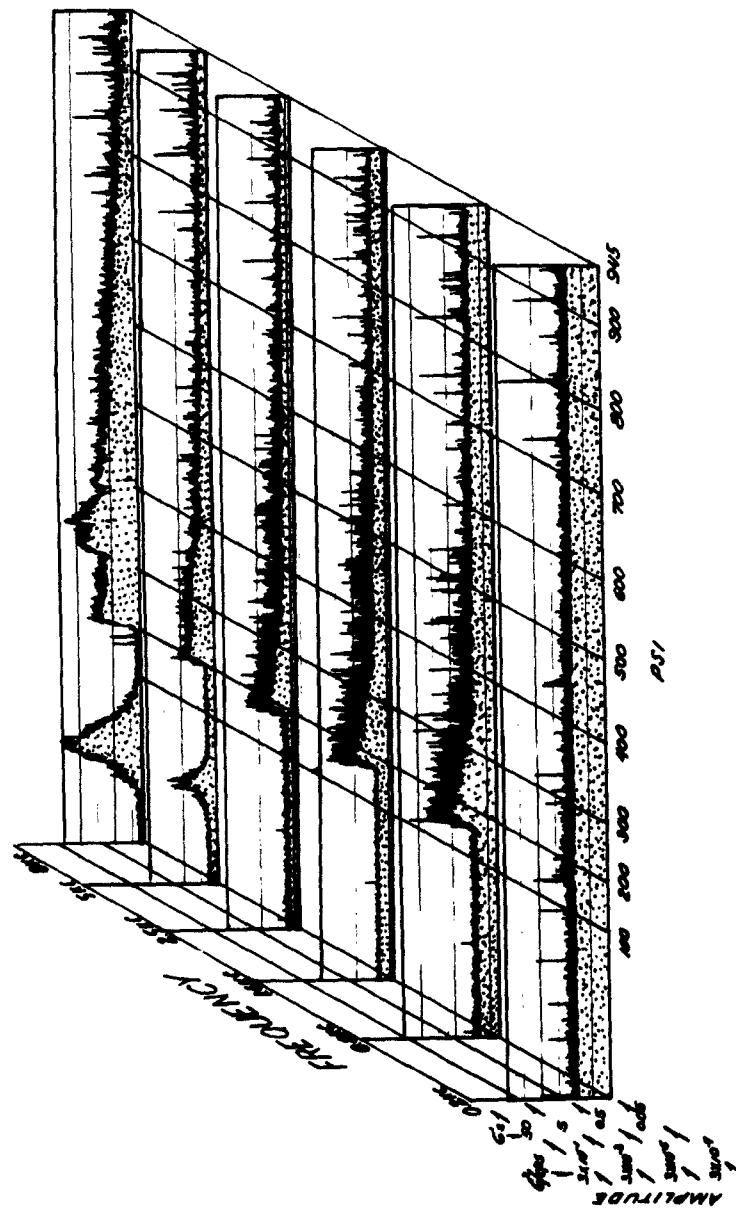| Accelerometer Function	Acceleration Amplitude at 0 psi (Peak G)	Acceleration Amplitude at 700 psi (Peak G)
G1	22.0	27.0
G2	6.9	11.0
G3	5.1	6.0
G4	1.3	1.6
G5	0.7	1.3
G6	0.6	0.9
G7	0.5	0.7
G8	0.3	0.6

Table 3

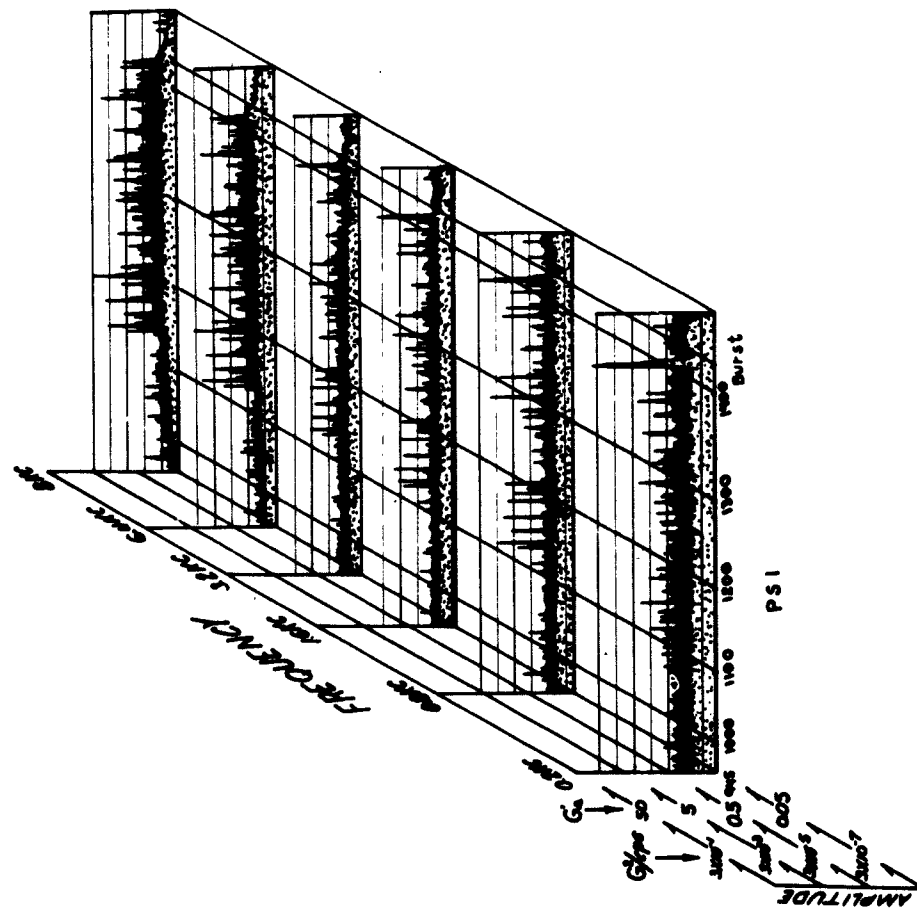Figure 1

Acceleration-Magnitude Surface Plot, Proof Test 645P

Figure 2

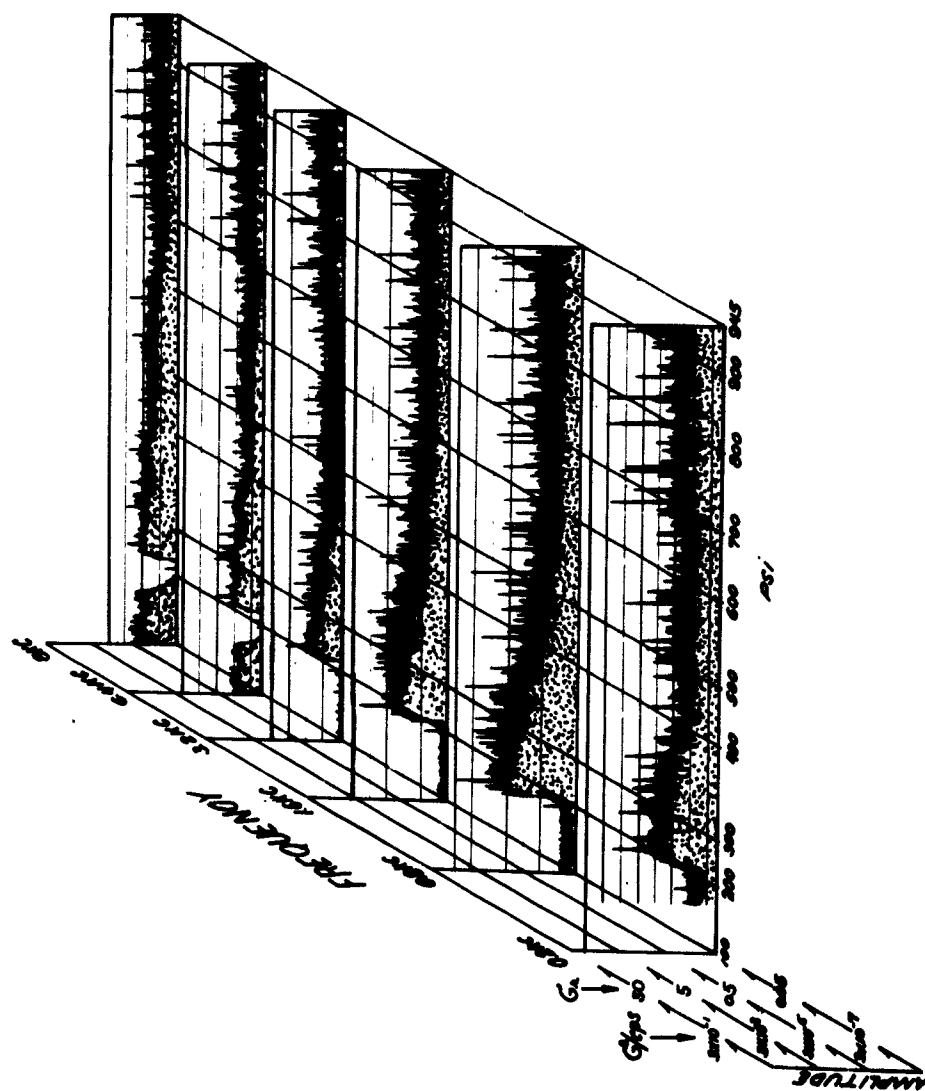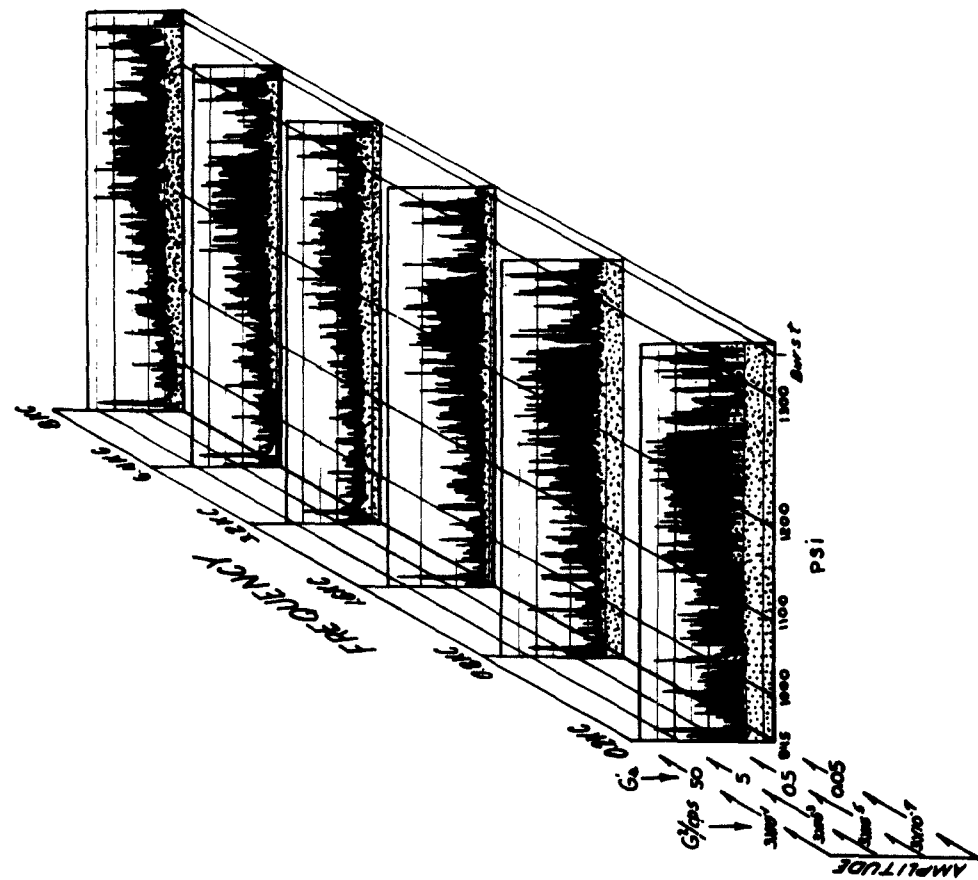Acceleration-Magnitude Surface Plot, Burst Test 645P

Figure 3

Acceleration-Magnitude Surface Plot, Proof Test 646P

Figure 4

Acceleration-Magnitude Surface Plot, Burst Test 646P

Figure 5

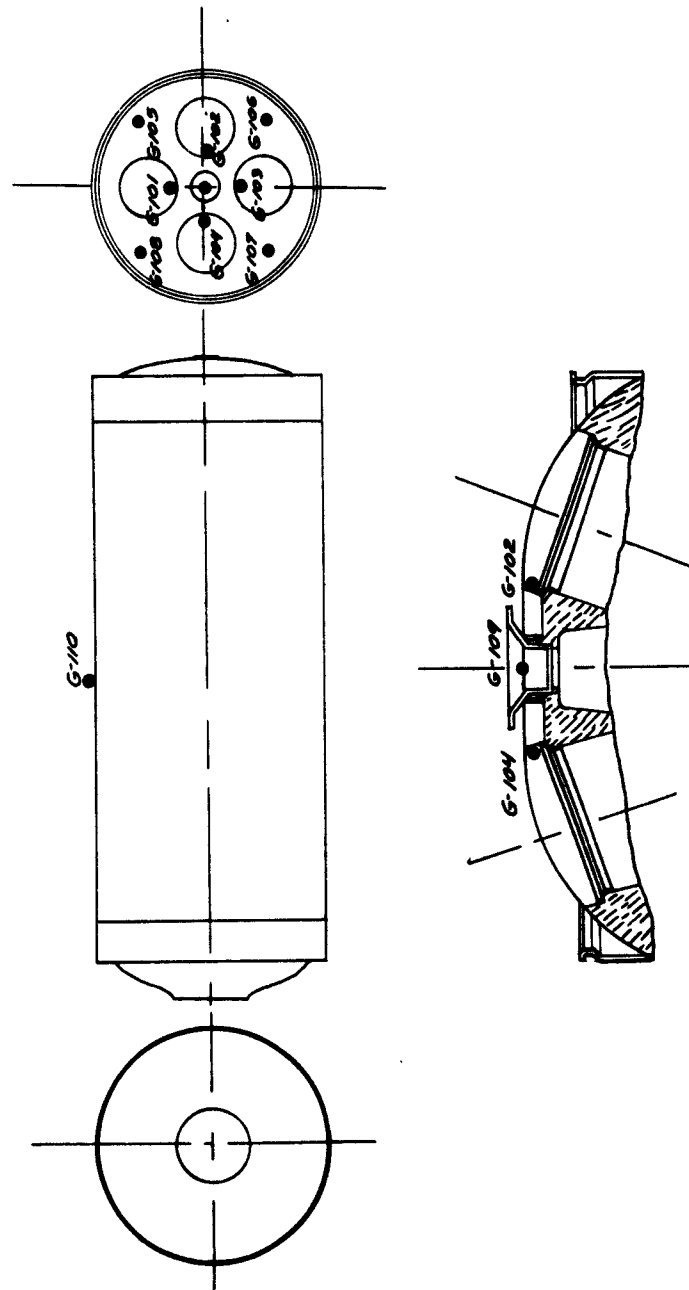Accelerometer Locations, Hydrostatic Test

Figure 6

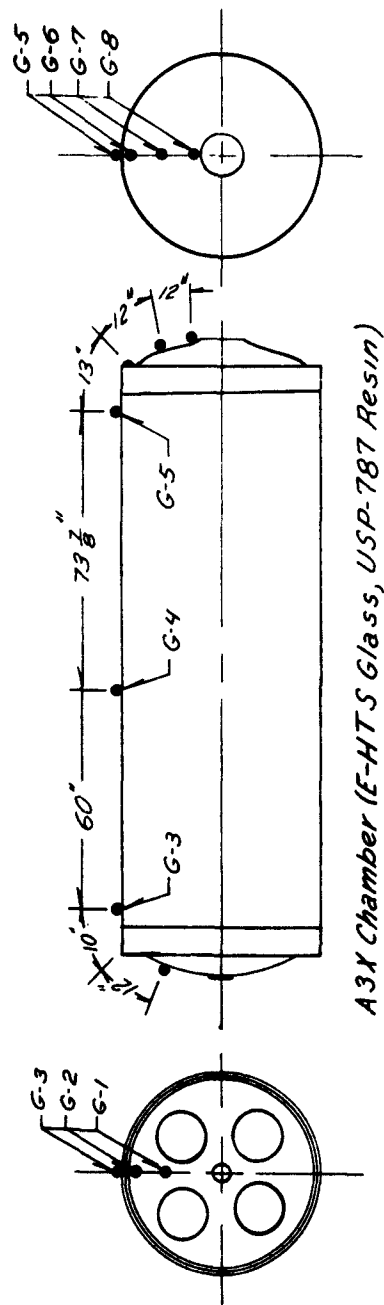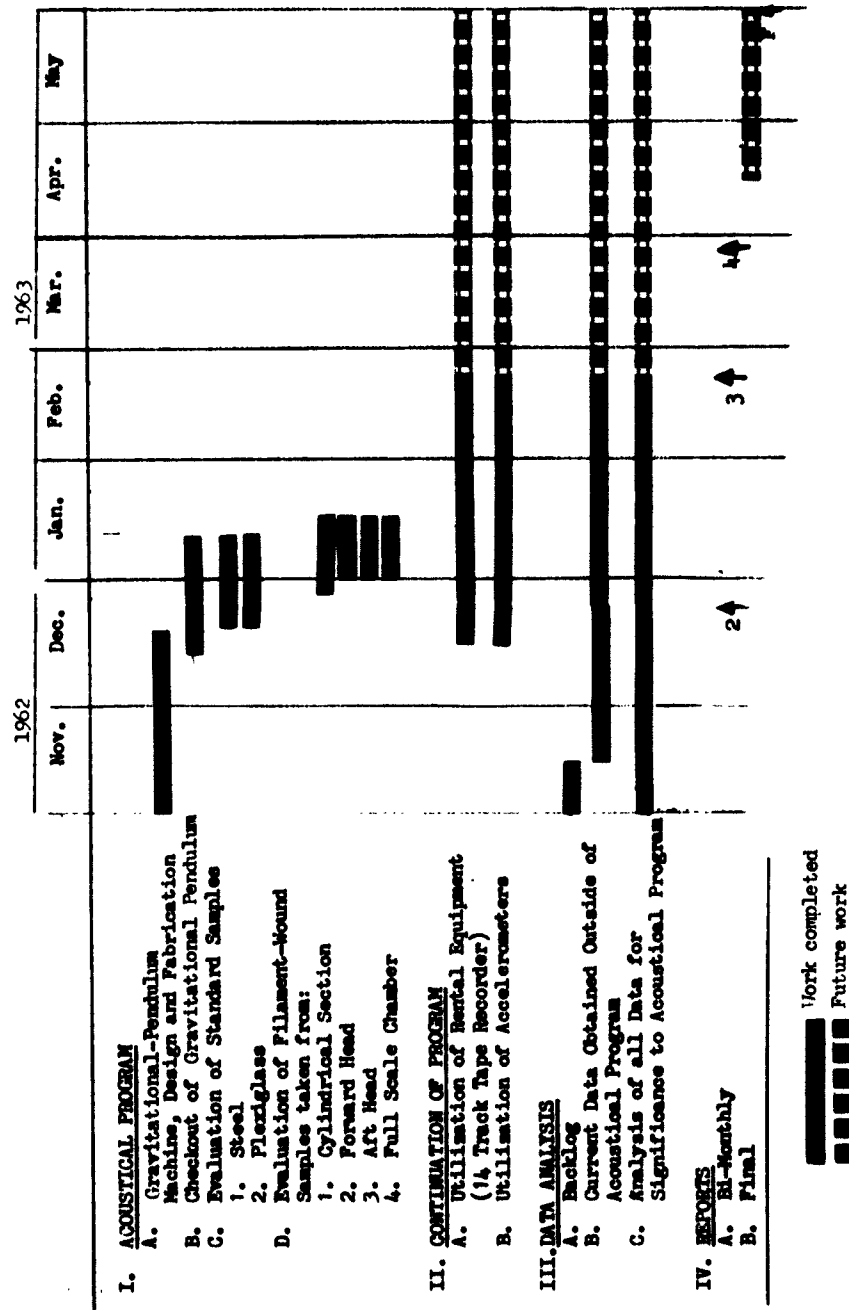A3X Chamber (E-HTS Glass, USP-787 Resin)

Accelerometer Locations, Chamber Shock-Transfer Characteristics

Figure 7

Time Schedule, Acoustics Program

Figure 8

APPENDIX A

INSTRUMENTATION, PHASE I

I. DATA-ACQUISITION SYSTEM

A block diagram of the data-acquisition system is shown in Figure 1. The operational characteristics of the system and the adequacy of the data acquired have proved acceptable.

The Electra Scientific Model ES-6016 accelerometers have a constant voltage output within $\pm$ 1 db from 5 to 40,000 cps. These accelerometers were used exclusively until subsequent data playback through the Brüel and Kjaer (B&K) filter system showed the data amplitude to be relatively flat over the 40,000-cps frequency spectrum. This analysis led to the use of the Columbia Model 302-8 accelerometer, which has a constant voltage output within $\pm$ 1 db from 5 to 8000 cps and which has proved more rugged and versatile than the Electra Model ES-6016.

The hydrostatic proof-pressure tests are currently instrumented with nine Model 302-8 and one Model ES-6016 accelerometers. The Model ES-6016 accelerometer is used as a standard to continuously verify that the hydrostatic-test acceleration amplitude is flat over the 40,000-cps frequency spectrum.

II. DATA-PLAYBACK SYSTEM

A block diagram of the data-playback system is also shown in Figure 1. The frequency content of the data determines if 1/3 octave or full-octave filtering is selected. If the data are gaussian, i.e., have a flat amplitude over the frequency spectrum, full-octave filters with wide bandwidths are used. If the data show discrete-frequency content, then the 1/3-octave filters with narrow band-widths are used.

At the beginning of the acoustical program, 1/3-octave filtering was used because it was suspected that the filament-wound chambers released discrete
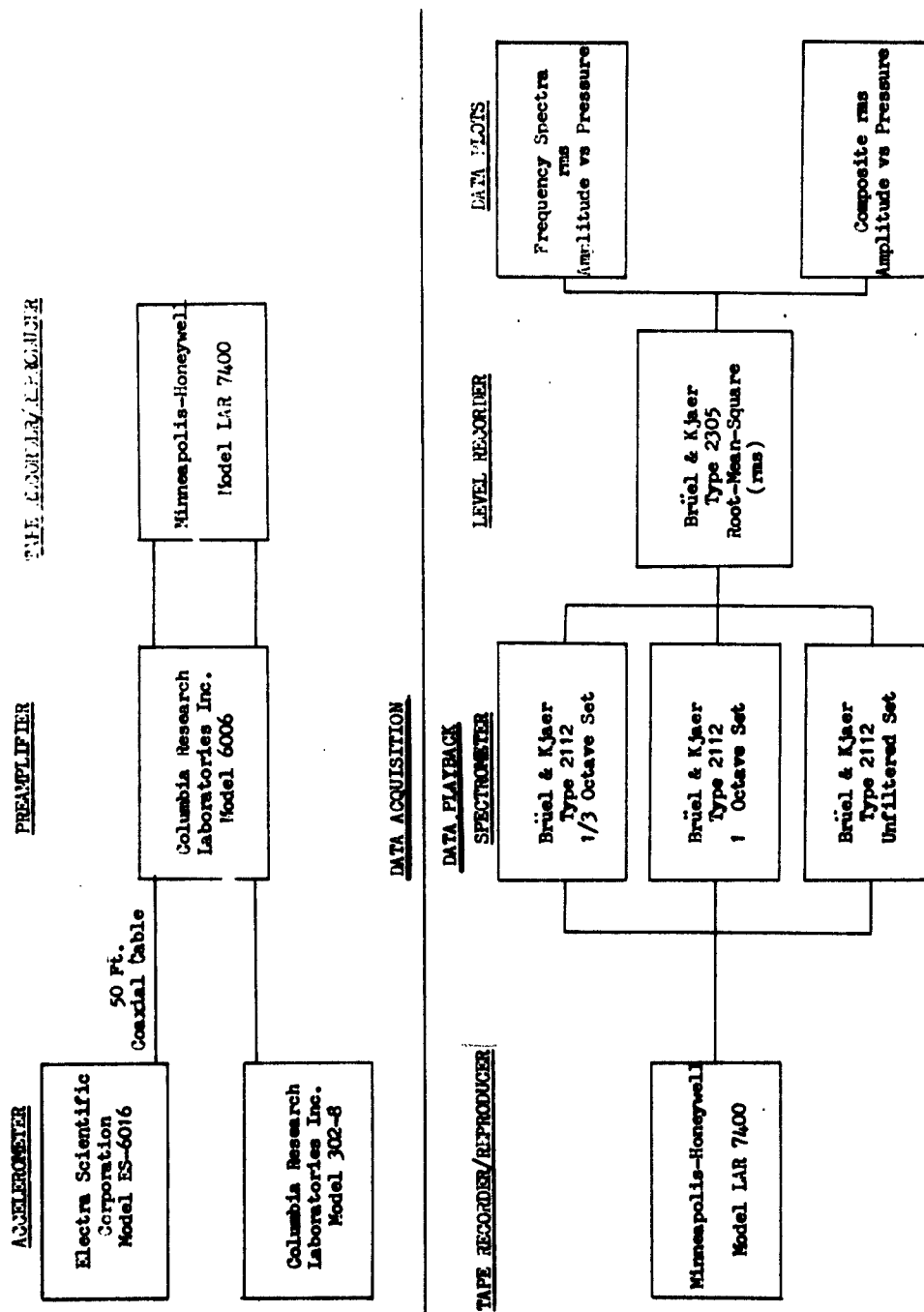
II, Data-Playback System (cont.)

frequencies during hydrostatic testing. At that time, the total frequency
spectrum of 180 to 9330 cps was investigated with 16 separate 1/3-octave
filters.

This investigation showed that the data amplitude was relatively flat
over the aforementioned frequency spectrum. The same investigation showed
that the entire frequency spectrum could be closely approximated by the use of
only six 1/3-octave filters. Since this investigation, the data have been filtered
through six filters during playback, thus greatly reducing the data-playback time.
The data-frequency content is periodically checked with all 16 filters to reaffirm
the validity of determining the overall frequency spectrum with only six filters.
Because the frequency spectrum is relatively flat, and no narrow frequency
bands have been detected (even for discrete events), the use of full-octave
filters has recently been initiated.

The raw accelerometer-data tapes are also played back through the B&K
system to display the raw data as unfiltered root-mean-square acceleration
amplitude vs pressure. These data plots are used in performing the data
correlative analysis between acceleration amplitude and chamber burst pressure.

The hydrostatic-test data indicate that the chamber structural-energy
release during hydrostatic pressure tests consists of a series of acceleration
impulses. These impulses occur at random intervals and acceleration amplitudes.
The B&K equipment averages the impulse amplitudes. When the impulse
density is low, the equipment averaging time is too short to plot an average
amplitude and the resultant data plot consists of a series of transient peaks.

ACCELEROMETER

Electra Scientific
Corporation
Model ES-6016

PREAMPLIFIER

50 Ft.
Coaxial Cable

Columbia Research
Laboratories Inc.
Model 6006

Columbia Research
Laboratories Inc.
Model 302-8

TAPE RECORDER/REPRODUCER

Minneapolis-Honeywell
Model LAR 7400

DATA ACQUISITION

TAPE RECORDER/REPRODUCER

Minneapolis-Honeywell
Model LAR 7400

DATA PLAYBACK
SPECTROMETER

Brüel & Kjaer
Type 2112
1/3 Octave Set

Brüel & Kjaer
Type 2112
1 Octave Set

Brüel & Kjaer
Type 2112
Unfiltered Set

LEVEL RECORDER

Brüel & Kjaer
Type 2305
Root-Mean-Square
(rms)

DATA PLOTS

Frequency Spectra
rms
Amplitude vs Pressure

Composite rms
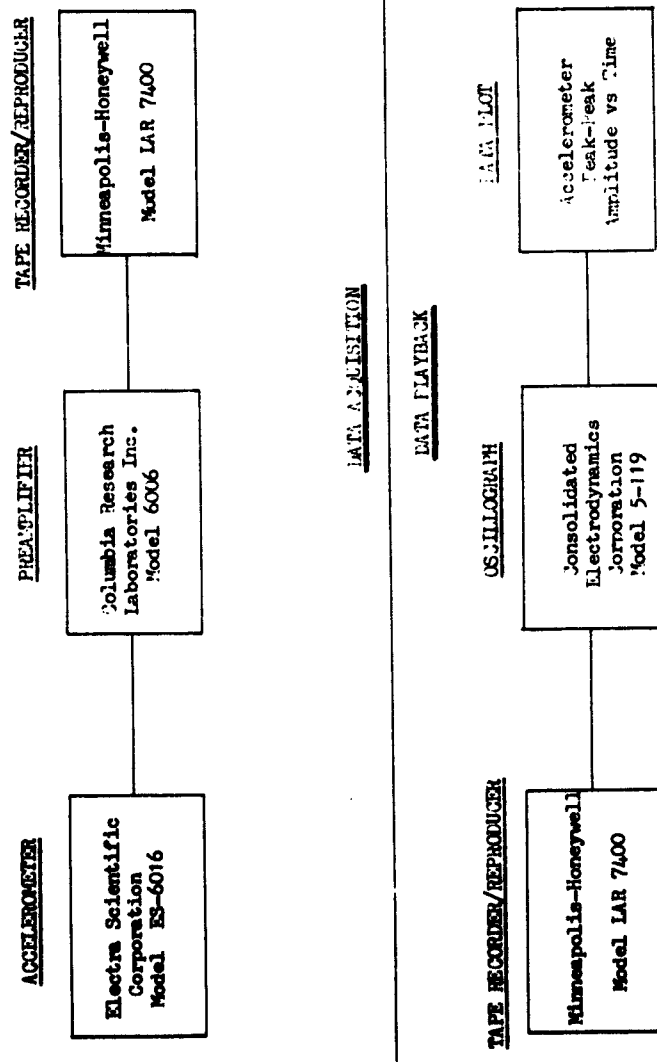Amplitude vs Pressure

Phase I, Instrumentation System

Figure 1

APPENDIX B

INSTRUMENTATION, PHASE II

DATA ACQUISITION AND PLAYBACK

A block diagram of the system used is shown in Figure 1. The recording system frequency response is 40,000 cps. The velocity-of-sound data were tape-recorded at a 60-in./sec tape speed and played back at a 0.6-in./sec tape speed. With the tape-recorder playback speed reduced by a factor of 100 and an oscillographic recorder speed of 160 in./sec, the effective oscillograph recording speed was 16,000 in./sec. This paper speed allows a time resolution of less than 2 microsec between data channels.

DATA ACQUISITION

DATA PLAYBACK

TAPE RECORDER/REPRODUCER

Minneapolis-Honeywell
Model LAR 7400

PREAMPLIFIER

Columbia Research
Laboratories Inc.
Model 6006

ACCELEROMETER

Electro Scientific
Corporation
Model ES-6016

DATA PLOT

Accelerometer
Peak-Peak
Amplitude vs Time

OSCILLOGRAPH

Consolidated
Electrodynamics
Corporation
Model 5-119

TAPE RECORDER/REPRODUCER

Minneapolis-Honeywell
Model LAR 7400

Phase II, Instrumentation System

Figure 1